

Microarray profiling of circular RNAs in steroid-associated osteonecrosis of the femoral head

Observational study

Tao Yao, MD^{a,b}, Zong-Sheng Yin, MD^{a,*}, Wei Huang, MD^{a,c}, Zhen-Fei Ding, MD^a, Chao Cheng, MD^a

Abstract

The aim of this study was to elucidate the molecular mechanisms and to identify the differential expression of circular RNAs (circRNAs) for steroid-associated osteonecrosis of the femoral head (SONFH) using bioinformatics analysis.

circRNA microarray was performed with 3 SONFH tissues and the adjacent normal tissues, and differentially expressed circRNA were identified by limma package in R. Gene ontology (GO) and Kyoto Encyclopedia of Genes and Genomes (KEGG) pathway enrichment analyses were performed using the Database for Annotation, Visualization and Integrated Discovery database. In addition, a differentially expressed genes (DEG)-associated circRNA/microRNA (miRNA) interaction was predicted by combination of TargetScan and miRanda, and the circRNA/miRNA interaction network generated by the cytoscape software.

A total of 647 differentially expressed circRNAs, including 433 upregulated and 214 downregulated circRNA were identified. The most enriched GO terms for upregulated and downregulated circRNA were extracellular matrix organization and leukocyte activation in biological process; extracellular matrix and spindle pole in cellular component; integrin binding and ATP binding in molecular function, and KEGG pathway enrichment analyses showed that the upregulated and downregulated circRNA were strongly associated with Protein digestion and absorption and Cell cycle. Moreover, a total of 212 differentially expressed messenger RNAs (mRNAs), including 113 upregulated and 99 downregulated genes were identified. In addition, from the analysis of miRNA, long noncoding RNAs, mRNA, and circRNA networks, we found that hsa_circ_0008136 and hsa_circ_0074758 were respectively the upregulated and downregulated circRNA with highest degrees.

The identified circRNA and mRNA could be implicated in the progression of human SONFH. The findings could lead to a better understanding of SONFH pathogenesis.

Abbreviations: BMSCs = bone marrow mesenchymal stem cells, BP = biological process, CC = cellular component, ceRNAs = competing endogenous RNAs, circRNAs = circular RNAs, GO = gene ontology, KEGG = Kyoto Encyclopedia of Genes and Genomes, MF = molecular function, miRNA = microRNA, MREs = miRNA response elements, MRI = magnetic resonance imaging, ncRNAs = noncoding RNAs, SONFH = osteonecrosis of the femoral head.

Keywords: differentially expressed gene, functional enrichment analysis, mRNA-miRNA-lncRNA-circRNA network, steroid-associated osteonecrosis of the femoral head

1. Introduction

Osteonecrosis of the femoral head (ONFH) is a multifactorial and disabling disease that involves multiple genetic and

environmental factors.^[1,2] Increased incidence of ONFH was reported over the past decade, and an estimated of 20,000 to 30,000 and 150,000 to 200,000 new cases of ONFH were respectively presented annually in the United States and China.^[3,4] Moreover, a total of 8.12 million ONFH patients in China remains a challenge to surgeons.^[5] As the main form of ONFH, steroid-associated osteonecrosis of the femoral head (SONFH) is one of the most common and severe complications following corticosteroid treatment.^[6,7] The pathogenic mechanisms of SONFH are correlated with impaired vascularization of the femoral head, resulting in partial ischemia and hypoxic status, followed by development of osteonecrosis.^[6,7] Due to high incidence and a large number of patients, elucidation of the potential molecular mechanisms contributing to the pathogenesis of SONFH is critical to identify potential target genes for the prevention and treatment of SONFH.

Human genome sequencing shows that although only 3% of the human genome codes for proteins, 80% of the human genome are transcribed.^[8] The numbers of non-coding transcripts greatly exceed protein-coding messenger RNAs (mRNAs) and represent species complexity.^[9] Long noncoding RNAs (lncRNAs) are noncoding RNAs that are longer than 200 nucleotides that regulate diverse cellular functions.^[10] Aberrant levels of lncRNAs have also been reported in ONFH patients.^[11] Circular RNAs (circRNAs) are another class of noncoding RNAs

Editor: Yan Li.

The authors have no conflicts of interest to disclose.

Supplemental Digital Content is available for this article.

^a Department of Orthopaedics, The First Affiliated Hospital of Anhui Medical University, ^b Department of Orthopaedics, The First People's Hospital of Hefei, the Third Affiliated Hospital of Anhui Medical University, ^c Department of Orthopaedics, Anhui Provincial Hospital, Hefei, Anhui, China.

* Correspondence: Zong-Sheng Yin, Department of Orthopaedics, The First Affiliated Hospital of Anhui Medical University, Hefei, Anhui Province, China (e-mail: anhuiyzs@126.com).

Copyright © 2020 the Author(s). Published by Wolters Kluwer Health, Inc. This is an open access article distributed under the terms of the Creative Commons Attribution-Non Commercial License 4.0 (CCBY-NC), where it is permissible to download, share, remix, transform, and buildup the work provided it is properly cited. The work cannot be used commercially without permission from the journal.

How to cite this article: Yao T, Yin ZS, Huang W, Ding ZF, Cheng C. Microarray profiling of circular RNAs in steroid-associated osteonecrosis of the femoral head: Observational study. *Medicine* 2020;99:10(e19465).

Received: 24 January 2019 / Received in final form: 4 January 2020 / Accepted: 5 February 2020

<http://dx.doi.org/10.1097/MD.00000000000019465>

that regulate gene expression in eukaryotes.^[12] The circRNAs are competing endogenous RNAs (ceRNAs) that act as a sponge for microRNAs (miRNAs) by complementary base pairing and therefore regulate gene transcription.^[13] However, the expression and biological functions of circRNAs in SONFH are unknown. Therefore, in the present study, we generated circRNAs expression profiles of 3 pairs of SONFH tissues and the adjacent normal tissues (NLs) to investigate their potential role as diagnostic markers in SONFH.

2. Materials and methods

2.1. Patients

Femoral heads were obtained from 3 patients who had corticosteroid usage histories and fulfilled the diagnosis of ONFH according to the guidelines of the Chinese Medical Association who were undergoing total hip arthroplasty at the Anhui Provincial Hospital (Hefei, China). The characteristics of the patients were listed in Supplementary Table S1, <http://links.lww.com/MD/D912>. Femoral heads were cut along the coronal plane to differentiate the osteonecrosis zone and normal zone according to previous description,^[14] which were defined as a pair group. After that, tissues of each zone were cut into small pieces of approximately $5 \times 5 \times 5 \text{ mm}^3$, and stored in a -80°C freezer. This study was carried out in accordance with the approved institutional guidelines, and the protocol was reviewed and approved by the Ethical Committee of the Anhui Provincial Hospital. Written informed consent was obtained from all patients.

2.2. Microarray analysis

Total RNA was extracted from the plasma of the subjects and purified using the RNeasy micro kit (Cat#74004, QIAGEN, GmbH, Germany) following the manufacturer's instructions. The RNA integration number was determined by an Agilent Bioanalyzer 2100 (Agilent technologies, Santa Clara, CA). Total RNA (1 μg) was amplified and labeled by Low Input Quick Amp Labeling Kit, One-Color (Cat.# 5190–2305, Agilent technologies) according to the manufacturer's instructions. Labeled cRNA were purified by RNeasy mini kit (Cat.# 74106, QIAGEN).

Each slide was hybridized with 1.65 μg Cy3-labeled cRNA using Gene Expression Hybridization Kit (Cat.# 5188-5242, Agilent technologies) in Hybridization Oven (Cat.# G2545A, Agilent technologies), according to the manufacturer's instructions. After 17 hours hybridization, slides were washed in staining dishes (Cat.# 121, Thermo Shandon, Waltham, MA) with Gene Expression Wash Buffer Kit (Cat.# 5188–5327, Agilent technologies), followed the manufacturer's instructions.

Slides were scanned by Agilent Microarray Scanner (Cat#G2565CA, Agilent technologies) with default settings, Dye channel: Green, Scan resolution = 3 μm , photoelectric multiplication tube 100%, 20bit. Data were extracted with Feature Extraction software 12.0 (Agilent technologies). Quantile normalization and subsequent data processing were performed using using a \log_2 ratio in R software package (provided by Biotechnology Corporation, China). Differentially expressed circRNAs between 2 groups with statistical significance were defined as fold changes ≥ 2 and Student *t* test *P*-values $< .05$. Those differentially expressed circRNAs were showed via Volcano Plot and Fold Change filtering. Hierarchical Clustering was applied to demonstrate the distinguishable circRNA expression profile among samples.

2.3. GO and KEGG pathway analysis of parental genes

Gene Ontology (GO) analysis, covering 3 different aspects namely biological process (BP), cellular component (CC), and molecular function (MF), was performed to explore the potential functions of the circRNA host genes and mRNA. Kyoto Encyclopedia of Genes and Genomes (KEGG) pathway analysis was carried out to detect the involvement of parental gene in the biological pathways. The top 10 enriched GO terms and pathways among the 2 groups were ranked by enrichment score ($-\log_{10}$ (*P*-value)) identified by Database for Annotation, Visualization and Integrated Discovery (<http://www.david.abcc.ncifcrf.gov/>).

2.4. Prediction of circRNA-miRNA interactions

The circRNA/miRNA interaction was predicted by combination of TargetScan and miRanda, with the principle of at least a perfect seed match. Based on the prediction of miRNA binding sites, the correlations between circRNA and miRNA were further analyzed by the circRNA/miRNA interaction network generated by the cytoscape software.

3. Results

3.1. Expression pattern of circRNA

To study the expression pattern of circRNAs in SONFH tissues (ONs) and the adjacent NLs, we performed the circRNA microarray to determine the differentially expressed circRNAs. The box plot showed that after \log_2 normalization, no abnormal distributions of data were found in the 6 samples (Fig. 1A). The variation between osteonecrosis tissues and matched NLs was observed in the scatter plot of circRNA expression profile (Fig. 1B). And the volcano plot identified differentially expressed circRNAs at different *P* values and fold-change between 2 groups (Fig. 1C). Hierarchical clustering revealed that circRNAs expression levels were distinguishable (Fig. 1D). There were 647 differentially expressed circRNAs (fold change ≥ 2.0 and $P < .05$) among these 2 cell groups, in which 433 circRNAs were found to be upregulated and 214 circRNAs were downregulated in ONs. In present study, the top 10 upregulated and downregulated circRNAs were summarized in Table 1 based on fold change.

3.2. Differentially expressed mRNAs

There were 212 differentially expressed mRNAs (fold change ≥ 2.0 and $P < .05$) among these 2 cell groups, in which 113 mRNAs were found to be upregulated and 99 mRNAs were downregulated in osteonecrosis tissues. In present study, the top 10 upregulated and downregulated mRNAs were summarized in Table 2 based on fold change.

3.3. GO and pathway analysis of the parental gene of circRNAs

The top 10 dysregulated GO analysis of each domain (BP, CC, and MF) were made according to enriched dysregulated circRNAs between ONs and NLs. GO terms with *P*-value $< .05$ were selected and ranked by enrichment score ($-\log_{10}$ [*P*-value]).

For the upregulated circRNAs, the top 3 enriched GO terms were extracellular matrix organization, extracellular structure

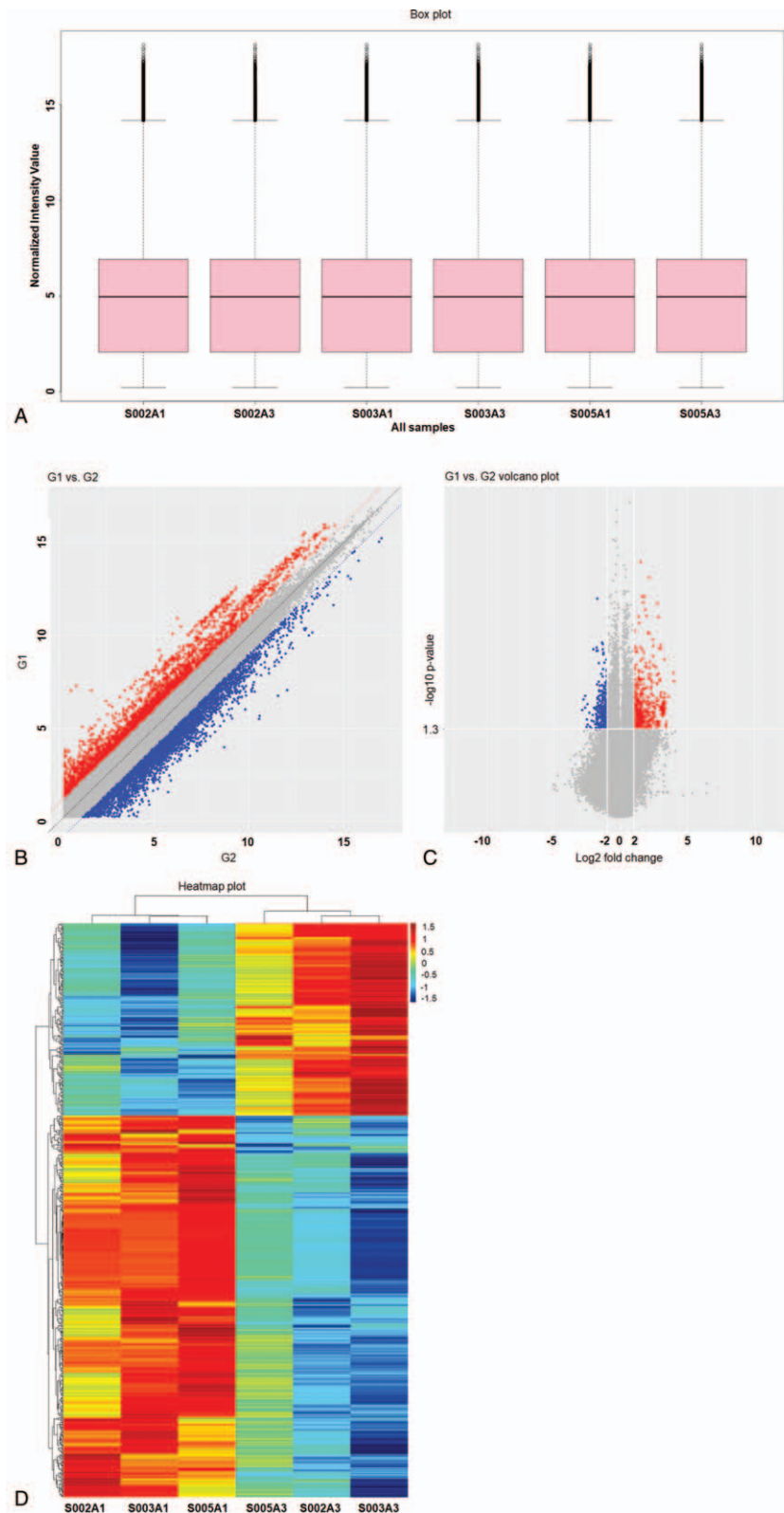


Figure 1. Expression profile of circRNAs detected by microarray in SONFH tissues (ONs) and the adjacent normal tissues (NLs). (A) The box plots are applied to visualize the distributions of circRNAs for 2 groups. After normalization, the distributions of log₂ ratios among 6 samples were nearly the same. (B) Scatter plots are used to evaluate the expression variation of circRNAs between ONs and NLs. The values of X and Y axes are the averaged normalized signal values of each group (log₂ scaled). The middle green line represents no difference between 2 groups. The circRNAs above the top green line and below the bottom green line indicate >2.0 fold changes between 2 groups. (C) Volcano plots show the differentially expressed circRNAs between 2 groups. The vertical lines correspond to 2.0 fold (log₂ scaled) up and down, respectively, and the horizontal line represents the P value of .05 ($-\log_{10}$ scaled). The red and blue points in plot represent the upregulated and downregulated circRNAs with statistical significance, respectively. (D) Hierarchical clustering shows a distinguishable expression profile of circRNAs between 2 groups. The values correspond to the different colors represent the fold change (log₂ transformed) of each sample. circRNAs = circular RNAs.

Table 1**The top 20 upregulated and downregulated circRNAs in SONFH tissues (ONs) and the adjacent normal tissues (NLs).**

CircRNA	P-value	Fold change	Regulation	Gene symbol	Chromosomes location
hsa_circ_0010027	.00976061	16.7088849	Up	PDPN	chr1
hsa_circ_0058115	.007376925	15.91280829	Up	FN1	chr2
hsa_circ_0010026	.016613654	12.5452502	Up	PDPN	chr1
hsa_circ_0058839	.046838844	10.88414736	Up	COL6A3	chr2
hsa_circ_0056886	.039763668	10.81230384	Up	FAP	chr2
hsa_circ_0056885	.041942917	10.60008116	Up	FAP	chr2
hsa_circ_0058146	.024393796	10.31947205	Up	FN1	chr2
hsa_circ_0058105	.020081631	10.30198198	Up	FN1	chr2
hsa_circ_0058112	.021205085	10.29226706	Up	FN1	chr2
hsa_circ_0058143	.014971728	10.21721226	Up	FN1	chr2
hsa_circ_0030528	.017007398	6.942966553	Down	SLAIN1	chr13
hsa_circ_0072575	.024771717	6.446280884	Down	DEPDC1B	chr5
hsa_circ_0012524	.016018604	6.434588919	Down	ORC1	chr1
hsa_circ_0000208	.036496848	5.911150575	Down	TCONS_00018414	chr10
hsa_circ_0043525	.043434903	5.64405666	Down	CDC6	chr17
hsa_circ_0056615	.022876771	5.625984973	Down	CXCR4	chr2
hsa_circ_0087745	.049982373	4.83315902	Down	NR4A3	chr9
hsa_circ_0063397	.037673318	4.607367198	Down	GRAP2	chr22
hsa_circ_0030529	.030964135	4.324887867	Down	SLAIN1	chr13
hsa_circ_0000497	.042085358	3.806391054	Down	SLAIN1	chr13

organization, extracellular matrix disease in BP (Fig. 2A); extracellular matrix, proteinaceous extracellular matrix, collagen in CC (Fig. 2B); integrin binding, L-ascorbic acid binding, Rho guanyl-nucleotide exchange factor activity in MF (Fig. 2C). KEGG analysis showed the top 10 pathways associated with upregulated circRNAs, and the top 3 were Protein digestion and absorption; extracellular matrix (ECM)-receptor interaction; focal adhesion; arrhythmogenic right ventricular cardiomyopathy (Fig. 2D).

For the downregulated circRNAs, the top 3 enriched GO terms were leukocyte activation, cell activation, lymphocyte activation in BP (Fig. 3A); spindle pole, actin cytoskeleton, endocytic vesicle in CC (Fig. 3B); ATP binding, adenylyl nucleotide binding,

phosphotransferase activity, alcohol group as acceptor in MF (Fig. 3C). KEGG analysis showed the top 10 pathways associated with downregulated circRNAs, and the top 3 were cell cycle; phosphatidylinositol signaling system; leukocyte transendothelial migration (Fig. 3D).

3.4. GO and pathway analysis of the parental gene of mRNAs

The top 10 dysregulated GO analysis of each domain (BP, CC, and MF) were made according to enriched dysregulated mRNAs between ONs and NLs. GO terms with P -value < .05 were selected and ranked by enrichment score ($-\log_{10}$ [P -value]).

Table 2**The top 20 up-regulated and down-regulated mRNAs in SONFH tissues (ONs) and the adjacent normal tissues (NLs).**

mRNA	P-value	Fold change	Regulation	Accession	Source	Chromosomes location
LNCV6_138395_P1430048170	.031859153	149.1536688	Up	NM_001844	RefSeq	chr12
LNCV6_144726_P1430048170	.03334352	101.5988634	Up	NM_007015	RefSeq	chr13
LNCV6_75716_P1430048170	.035983983	91.74341624	Up	NM_001884	RefSeq	chr5
LNCV6_141888_P1430048170	.006874178	34.52682484	Up	NM_001166034	RefSeq	chr19
LNCV6_135071_P1430048170	.035558634	28.57583967	Up	NM_013372	RefSeq	chr15_K1270905v1_alt
LNCV6_145585_P1430048170	.025594129	27.93413372	Up	NM_007281	RefSeq	chr4
LNCV6_139705_P1430048170	.036450376	23.81068051	Up	NM_024746	RefSeq	chr1
LNCV6_137528_P1430048170	.015386026	23.22171806	Up	NM_000095	RefSeq	chr19
LNCV6_140132_P1430048170	.027965374	20.06038048	Up	NM_207419	RefSeq	chr16
LNCV6_126941_P1430048170	.028654319	17.45121797	Up	NM_006474	RefSeq	chr1
LNCV6_73320_P1430048170	.046893765	7.462652829	Down	NM_018189	RefSeq	chr3
LNCV6_63460_P1430048170	.045052269	6.692911528	Down	NM_001162995	RefSeq	chr17
LNCV6_140024_P1430048170	.017260387	6.434854886	Down	NM_001281834	RefSeq	chr1
LNCV6_141536_P1430048170	.04255825	6.342924893	Down	NM_017688	RefSeq	chr9
LNCV6_100478_P1430048170	.04101872	6.019934982	Down	NM_182538	RefSeq	chr17
LNCV6_144813_P1430048170	.046425605	5.190341779	Down	NM_022893	RefSeq	chr2
LNCV6_126919_P1430048170	.024335874	4.953649162	Down	NM_145719	RefSeq	chr11
LNCV6_141354_P1430048170	.043128303	4.58740727	Down	NM_001261430	RefSeq	chr17
LNCV6_129889_P1430048170	.020784577	4.361486679	Down	NM_080759	RefSeq	chr13
LNCV6_135847_P1430048170	.03476525	4.328064358	Down	NM_001282775	RefSeq	chr1

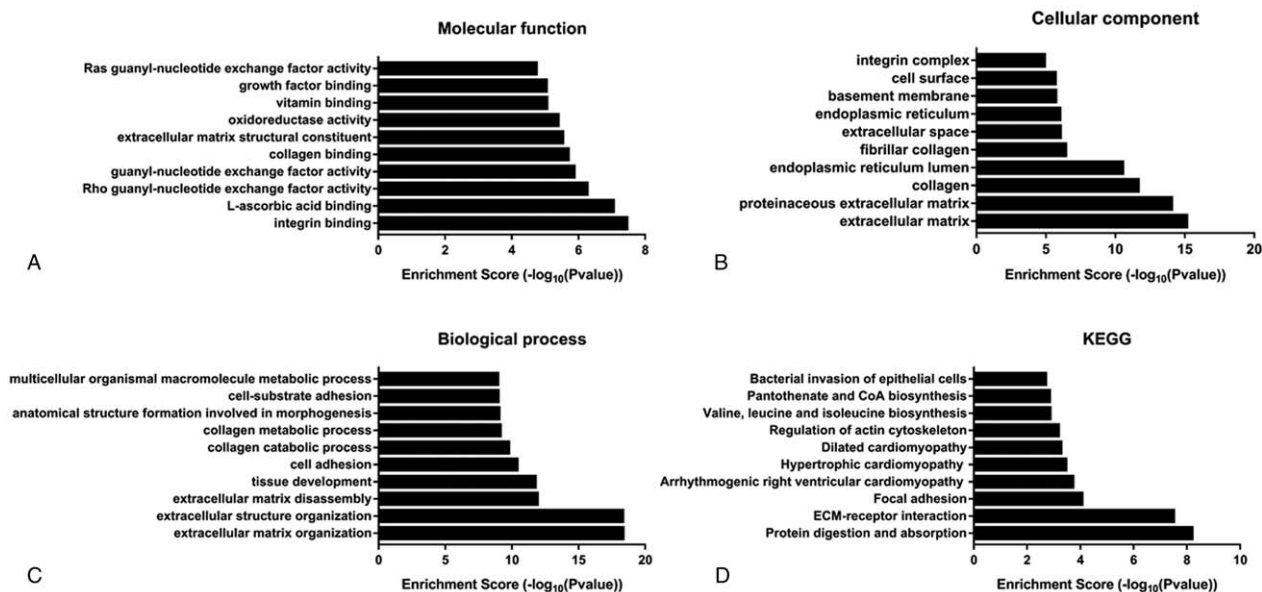


Figure 2. Gene ontology (GO) and KEGG analysis for upregulated circRNA host genes between SONFH tissues (ONs) and the adjacent normal tissues (NLs). Most significantly enriched GO terms in biological process (A), cellular component (B), molecular function (C), and KEGG pathway (D) corresponded to the upregulated circRNAs. circRNAs = circular RNAs, KEGG = Kyoto Encyclopedia of Genes and Genomes.

For the upregulated mRNAs, the top 3 enriched GO terms were tissue development, cartilage development, connective tissue development in BP (Fig. 4A); extracellular matrix, proteinaceous extracellular matrix, extracellular space in CC (Fig. 4B); heparin binding, glycosaminoglycan binding, extracellular matrix structural constituent in MF (Fig. 4C). KEGG analysis showed the top 10 pathways associated with upregulated mRNAs, and the top 3

were ECM-receptor interaction; Protein digestion and absorption; valine, leucine, and isoleucine biosynthesis (Fig. 4D).

For the downregulated mRNAs, the top 3 enriched GO terms were leukocyte activation, lymphocyte activation, cell activation in BP (Fig. 5A); external side of plasma membrane, plasma membrane, cell periphery in CC (Fig. 5B); heparin binding, glycosaminoglycan binding, extracellular matrix structural

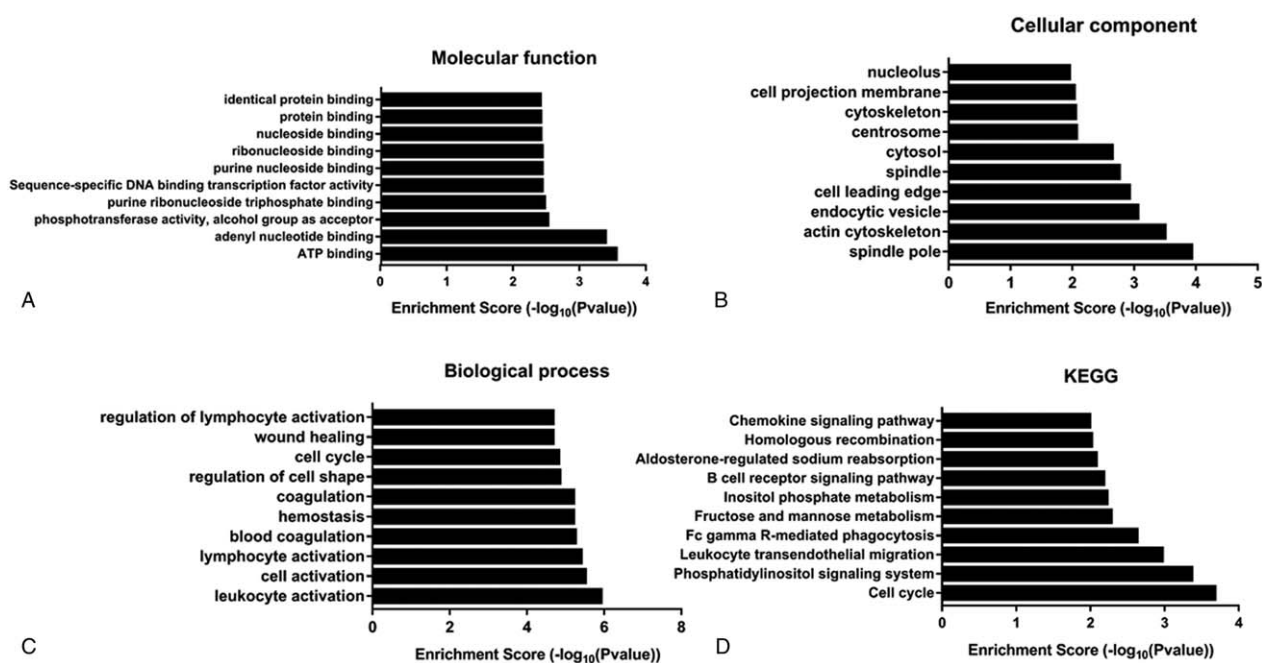


Figure 3. Gene ontology (GO) and KEGG analysis for downregulated circRNA host genes between SONFH tissues (ONs) and the adjacent normal tissues (NLs). Most significantly enriched GO terms in biological process (A), cellular component (B), molecular function (C), and KEGG pathway (D) corresponded to the downregulated circRNAs. circRNAs = circular RNAs, KEGG = Kyoto Encyclopedia of Genes and Genomes.

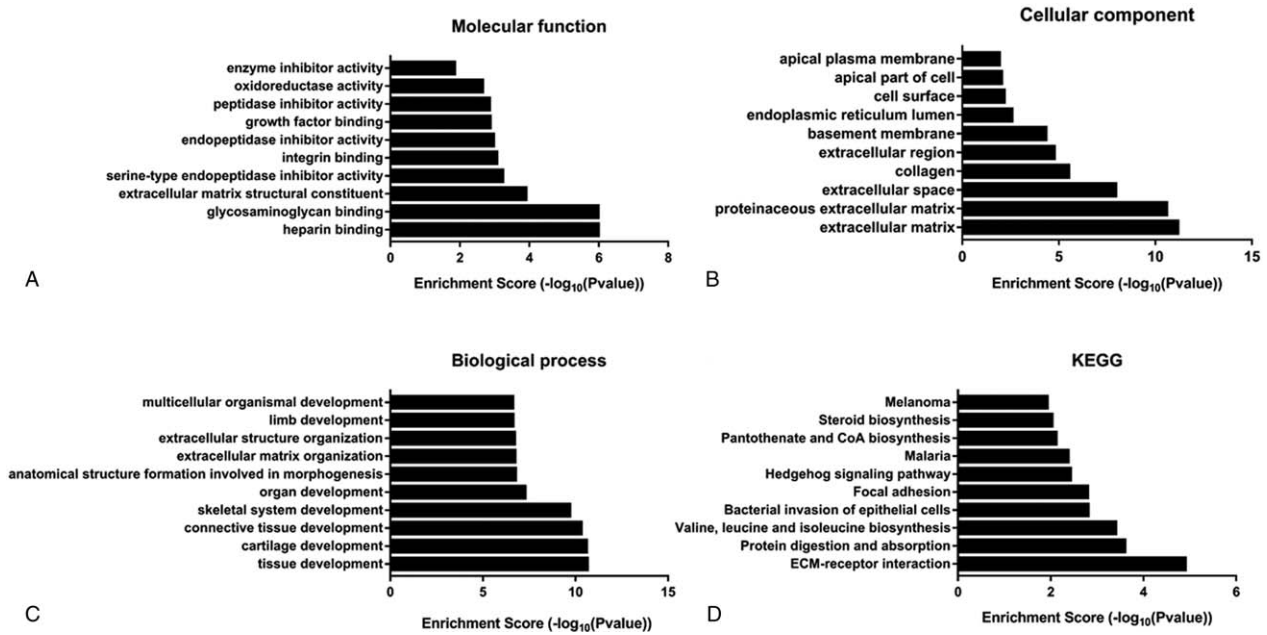


Figure 4. Gene ontology (GO) and KEGG pathway analysis for upregulated mRNA. Most significantly enriched GO terms in biological process (A), cellular component (B), molecular function (C), and KEGG pathway (D) corresponded to the upregulated mRNA. KEGG = Kyoto Encyclopedia of Genes and Genomes.

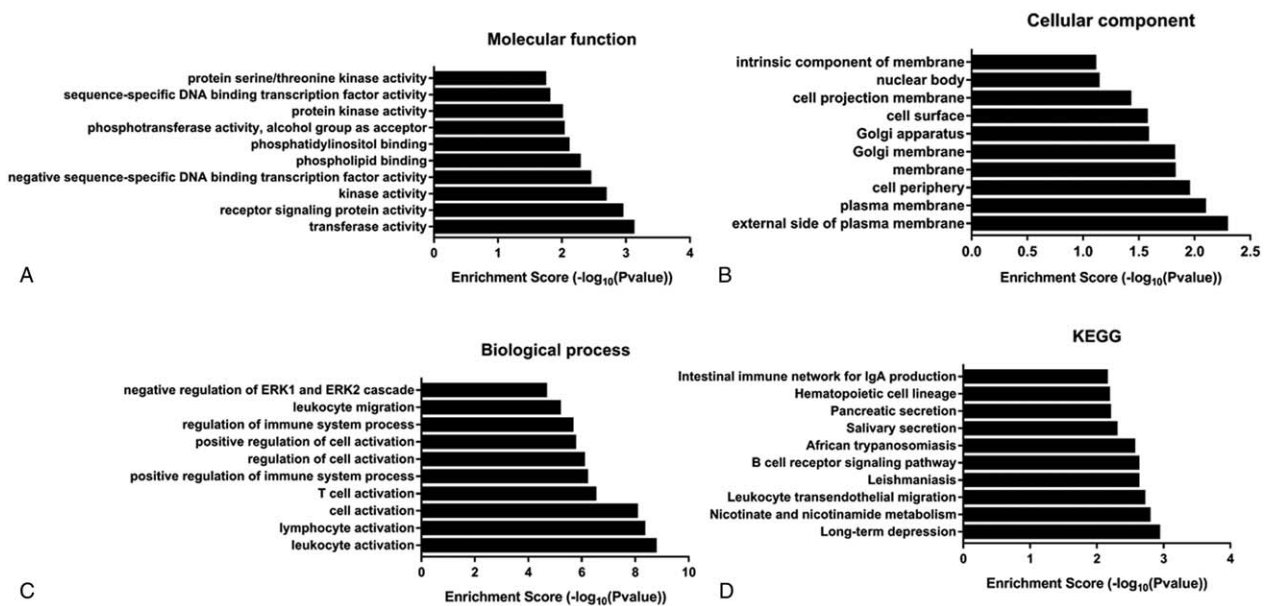


Figure 5. Gene ontology (GO) and KEGG pathway analysis for downregulated mRNA. Most significantly enriched GO terms in biological process (A), cellular component (B), molecular function (C), and KEGG pathway (D) corresponded to the downregulated mRNA. KEGG = Kyoto Encyclopedia of Genes and Genomes.

constituent in MF (Fig. 5C). KEGG analysis showed the top 10 pathways associated with downregulated mRNAs, and the top 3 were long-term depression; nicotinate and nicotinamide metabolism; leukocyte transendothelial migration (Fig. 5D).

3.5. Predicted miRNA response elements of top 20 upregulated and downregulated circRNA in ONs and NLs

We also predicted the miRNA response elements of top 20 upregulated and downregulated circRNA in ONs and NLs, and the results were listed in Table 3.

3.6. Overall regulatory network analysis of miRNA, circRNA, and mRNA

Differentially-expressed miRNA, circRNA, and mRNA were analyzed by Ingenuity Pathways Analysis for overall regulatory network analysis. Sub-networks with a high number of interactions are presented in detail in Figures 6 and 7. In the network, rhombus represents circRNA, circle represents mRNA and arrow represents miRNA, whereas, green represents downregulated, red represents upregulated, and yellow represents not determined. From numerous networks of mRNA-miRNA-circRNA, we listed

Table 3
The top 20 upregulated and downregulated circRNA and predicted miRNA response elements in SONFH tissues (ONs) and the adjacent normal tissues (NLs).

circRNA	P-value	Fold change	Regulation	circRNA_MRE1	circRNA_MRE2	circRNA_MRE3	circRNA_MRE4	circRNA_MRE5
hsa_circ_0010027	.00976061	16.7088849	Up	hsa-miR-1269a\$2	hsa-miR-1269b\$2	hsa-miR-4715-3p\$1	hsa-miR-4254\$1	hsa-miR-6733-3p\$1
hsa_circ_0058115	.007376925	15.91280829	Up	hsa-miR-1289\$3	hsa-miR-6880-5p\$3	hsa-miR-508-5p\$3	hsa-miR-1915-3p\$3	hsa-miR-6764-5p\$3
hsa_circ_0010026	.016613654	12.5452502	Up	hsa-miR-4254\$1	hsa-miR-6733-3p\$1	hsa-miR-4321\$1	hsa-miR-3622b-5p\$1	hsa-miR-6880-3p\$3
hsa_circ_0058839	.046838844	10.88414736	Up	hsa-miR-4663\$5	hsa-miR-4733-3p\$4	hsa-miR-3907\$3	hsa-miR-548q\$3	hsa-miR-3065-3p\$3
hsa_circ_0056886	.039763668	10.81230384	Up	hsa-miR-3158-5p\$1	hsa-miR-219a-5p\$1	hsa-miR-3974\$1	hsa-miR-182-3p\$1	hsa-miR-4782-3p\$1
hsa_circ_0056885	.041942917	10.60008116	Up	hsa-miR-2355-3p\$2	hsa-miR-676-3p\$2	hsa-miR-519e-5p\$2	hsa-miR-515-5p\$2	hsa-miR-885-5p\$2
hsa_circ_0058146	.024393796	10.31947205	Up	hsa-miR-1238-3p\$2	hsa-miR-1913\$2	hsa-miR-324-3p\$2	hsa-miR-181a-2-3p\$2	hsa-miR-515-5p\$2
hsa_circ_0058105	.020081631	10.30198198	Up	hsa-miR-1238-3p\$5	hsa-miR-4673\$5	hsa-miR-670-3p\$5	hsa-miR-532-3p\$4	hsa-miR-4713-5p\$4
hsa_circ_0058112	.021205085	10.29226706	Up	hsa-miR-532-3p\$6	hsa-miR-4713-5p\$5	hsa-miR-2116-3p\$5	hsa-miR-6880-5p\$4	hsa-miR-1289\$4
hsa_circ_0058143	.014971728	10.21721226	Up	hsa-miR-6756-5p\$2	hsa-miR-6766-5p\$2	hsa-miR-3161\$2	hsa-miR-181a-2-3p\$2	hsa-miR-7641\$2
hsa_circ_0030528	.017007398	6.942967	Down	hsa-miR-7854-3p\$1	hsa-miR-2115-5p\$1	hsa-miR-4433a-3p\$1	hsa-miR-3618\$1	hsa-miR-639\$1
hsa_circ_0072575	.024771717	6.446281	Down	hsa-miR-376a-3p\$2	hsa-miR-376b-3p\$2	hsa-miR-4762-5p\$2	hsa-miR-6878-3p\$1	hsa-miR-4757-5p\$1
hsa_circ_0012524	.016018604	6.434589	Down	hsa-miR-130b-5p\$2	hsa-miR-3692-5p\$2	hsa-miR-4314\$2	hsa-miR-4778-3p\$2	hsa-miR-216b-5p\$2
hsa_circ_0043525	.043434903	5.644057	Down	hsa-miR-3653-5p\$2	hsa-miR-1251-5p\$2	hsa-miR-198\$2	hsa-miR-517-5p\$2	hsa-miR-3176\$2
hsa_circ_0087745	.049982373	4.833159	Down	hsa-miR-3175\$1	hsa-miR-3150a-3p\$1	hsa-miR-6763-5p\$1	hsa-miR-5004-5p\$1	hsa-miR-6889-3p\$1
hsa_circ_0063397	.037673318	4.607367	Down	hsa-miR-149-5p\$2	hsa-miR-1538\$1	hsa-miR-4745-3p\$1	hsa-miR-939-5p\$1	hsa-miR-4641\$1
hsa_circ_0030529	.030964135	4.324888	Down	hsa-miR-5196-3p\$2	hsa-miR-491-5p\$2	hsa-miR-6881-3p\$2	hsa-miR-6134\$2	hsa-miR-4691-5p\$2
hsa_circ_0000497	.042085358	3.806391	Down	hsa-miR-7854-3p\$3	hsa-miR-6134\$3	hsa-miR-5196-3p\$2	hsa-miR-6881-3p\$2	hsa-miR-877-3p\$2
hsa_circ_0064395	.024810915	3.756149	Down	hsa-miR-3151-5p\$1	hsa-miR-185-3p\$1	hsa-miR-1204\$1	hsa-miR-939-3p\$1	hsa-miR-6796-5p\$1
hsa_circ_0063398	.029648282	3.630567	Down	hsa-miR-3907\$3	hsa-miR-6791-5p\$2	hsa-miR-4292\$2	hsa-miR-4731-5p\$2	hsa-miR-138-5p\$2

circRNAs = circular RNAs.

6 miRNAs with highest degree, which are miR-34c-5p; miR-378a-3p; miR-378g; miR-423-5p, miR-1268a, and miR-1268b.

4. Discussion

Current advances in gene microarray technology and bioinformatics analysis offer new opportunities to discover the functional genes for certain diseases. In the present study, 3 SONFH tissues and the adjacent NLs were obtained from the patients and differentially expressed circRNA and related mRNA were identified by microarray profiling. A total of 647 differentially expressed circRNAs, including 433 upregulated and 214 downregulated circRNA were identified. The most enriched GO terms were natural killer cell differentiation in BP; fibrillary collagen in CC; phosphate ion homestasis in MF, and KEGG pathway enrichment analyses showed that the dysregulated circRNA were strongly associated with valine, leucine, and isoleucine biosynthesis; ECM-receptor interaction; protein digestion and absorption. Moreover, a total of 212 differentially expressed mRNAs, including 113 upregulated and 99 downregulated genes were identified. The most enriched GO terms were endochondral bone morphogenesis in BP; microvillus membrane in CC; endochondral bone growth in MF, and KEGG pathway enrichment analyses showed that the dysregulated mRNA were strongly associated with valine, leucine, and isoleucine biosynthesis; ECM-receptor interaction; nicotinate and nicotinamide metabolism. Moreover, a total of 584 circRNAs were predicted to have the binding sites for miRNAs

circRNAs are new members of ceRNAs that are involved in regulating gene expression.^[15] However, their role in SONFH pathogenesis has not been reported. In the present study, we listed top 20 aberrantly expressed circRNAs (10 upregulated and 10 downregulated) in SONFH patients. These included hsa_circ_0010027, hsa_circ_0058115, hsa_circ_0010026, hsa_circ_0058839, hsa_circ_0056886, hsa_circ_0056885, hsa_circ_0058146, hsa_circ_0058105, hsa_circ_0058112, hsa_circ_0058143, hsa_circ_0030528, hsa_circ_0072575, hsa_circ_0012524, hsa_circ_0000208, hsa_circ_0043525, hsa_circ_0056615, hsa_circ_0087745, hsa_circ_0063397, hsa_circ_0030529, hsa_circ_0000497. There is limited but inconclusive evidence to support their roles in the development and progression of SONFH, which warrants further investigation.

GO and KEGG pathway analyses were performed to better understand the interactions of the dysregulated circRNA. In the present study, GO analyses showed that dysregulated circRNA were majorly involved in natural killer cell differentiation, endothelial cell differentiation, collagen catabolic process in BP; fibrillary collagen, integrin complex, collagen in CC; phosphate ion homestasis, L-ascorbic acid binding, protein hydroxylation in MF. Furthermore, KEGG pathways for the dysregulated circRNA were mainly related to valine, leucine, and isoleucine biosynthesis; ECM-receptor interaction; Protein digestion and absorption; pantothenate and CoA biosynthesis; sulfur metabolism; synthesis and degradation of ketone bodies. There were the novel discoveries by comparison with the previous reports about pathways that play important roles in the development and progression of SONFH.^[11,16-23]

Until now, few studies has focus on the expression profiling of human SONFH sample to uncover the possible mechanisms. Kerachian et al^[16] employed rat femoral heads with apoptosis signs after corticosteroid treatment, and performed exon array. Their results demonstrated a significant upregulation of 51 genes, and alpha-2-macroglobulin (A2M) gene was particularly over-expressed. After experimentation verification, they concluded that A2M as a potential marker, and a treatment target, for early SONFH. Moreover, abnormal bone marrow mesenchymal stem cells (BMSCs) transdifferentiation has been recognized as one of risk factor in SONFH. Wang et al^[17] evaluated dysregulated miRNAs in SONFH using mouse femoral head. Their results showed that 2 upregulated miRNAs: miR-21-3p and miR-652-5p and 5 downregulated miRNAs: miR-206-3p, miR-196a-5p, miR-34b-3p, miR-34c-5p, and miR-148a-3p. Here, we also found that dysregulated cirRNA hsa_circ_0069614 and hsa_circ_0006348 have miR-34b-3p binding sites. Moreover,

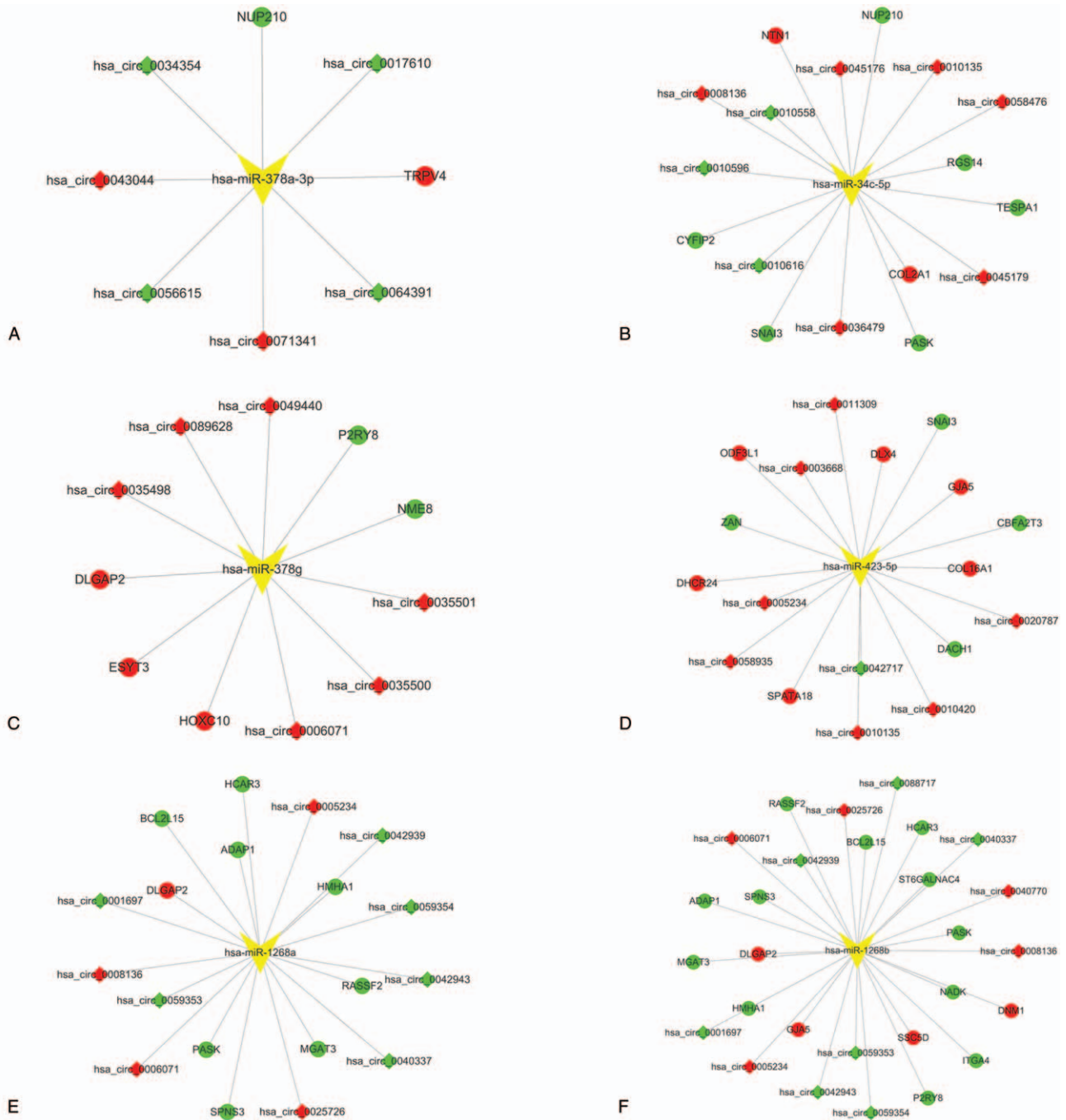


Figure 6. Overall regulatory network of miRNA, circRNA, and mRNA in SONFH tissues (ONs) samples. In the network, hombus represents circRNA, circle represents mRNA and arrow represents miRNA, whereas, green represents downregulated, red represents upregulated, and yellow represents not determined. A. miR-34c-5p; B. miR-378a-3p; C. miR-378g; D. miR-423-5p E. miR-1268a F. miR-1268b. circRNAs = circular RNAs, miRNA = microRNA.

dysregulated cirRNA hsa_circ_0064404, hsa_circ_0064402, and hsa_circ_0064394 have miR-34c-5p binding sites. Moreover, Wang et al^[11] recently investigated for the lncRNA expression profile of BMSCs from SONFH, and confirmed lncRNA RP1-193H18.2, MALAT1, and HOTAIR were associated with abnormal osteogenic and adipogenic differentiation of BMSCs in the patients with SONFH.

There were several limitations to the present study. First, the results were only analyzed using bioinformatics; experimental

verification is required to better confirm the findings of the identified genes and pathways in our investigation. Third, the sample size for the microarray analysis was relatively small. Only 6 3 SONFH and 3 matched control samples from 3 patients were obtained from the SONFH patients for bioinformatics analysis. It will be necessary to recruit more subjects in the future to get more accurate correlation results. A series of verification experiments must be performed based on a larger sample size to confirm our results.

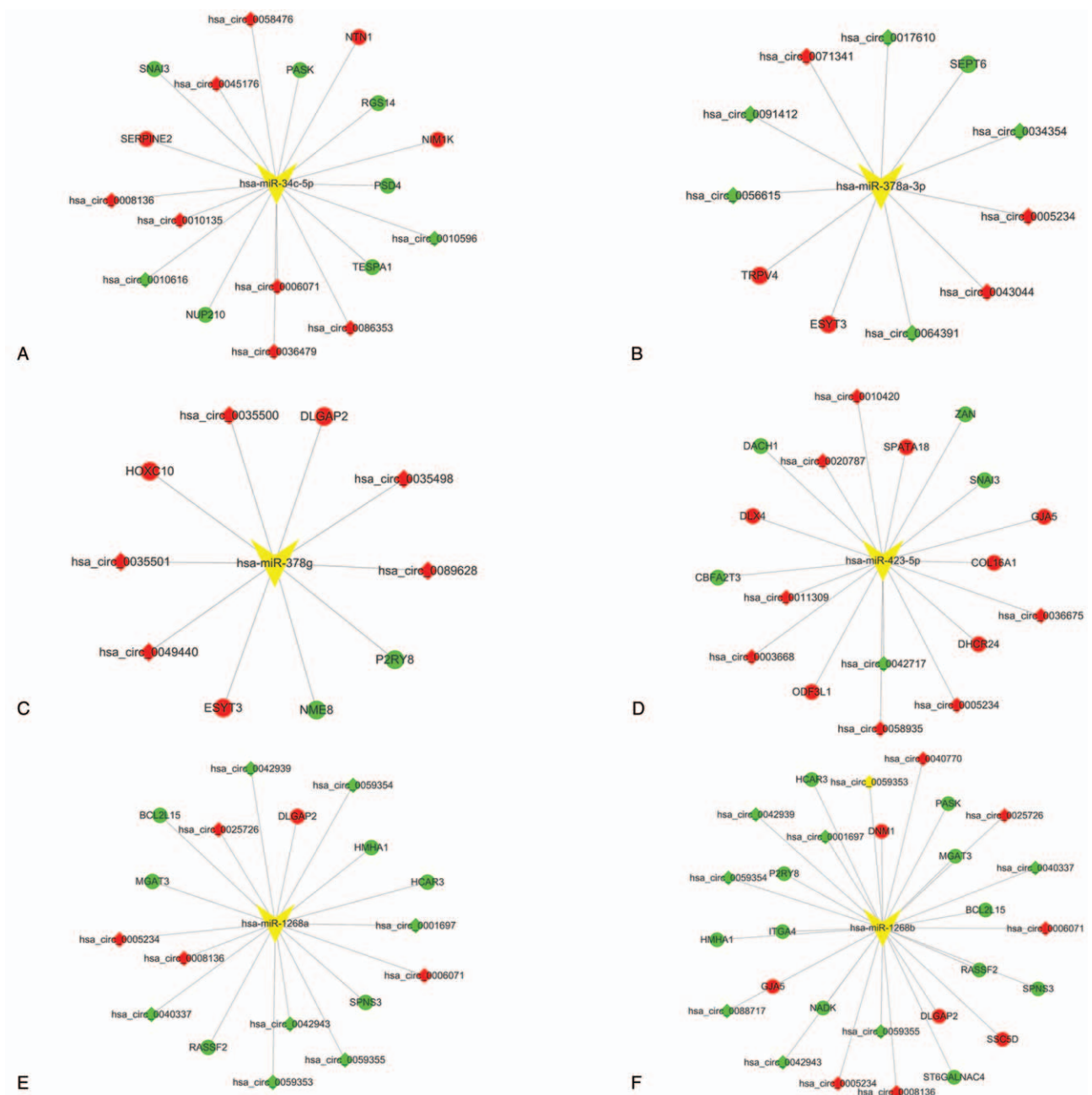


Figure 7. Overall regulatory network of miRNA, lncRNA, and mRNA in the adjacent normal tissues (NLT) samples. In the network, hombus represents circRNA, circle represents mRNA and arrow represents miRNA, whereas, green represents downregulated, red represents upregulated, and yellow represents not determined. (A) miR-34c-5p; (B) miR-378a-3p; (C) miR-378g; (D) miR-423-5p; (E) miR-1268a; (F) miR-1268b. circRNAs = circular RNAs, miRNA = microRNA.

In summary, we identified several new key circRNA, mRNA, pathways, and circRNA/miRNA interaction closely associated with SONFH using a series of bioinformatics analyses on DEGs between SONFH samples and control samples. The key upregulated circRNAs, including hsa_circ_0010027, hsa_circ_0058115, and hsa_circ_0010026, and key downregulated circRNAs, including hsa_circ_0030528, hsa_circ_0072575, and hsa_circ_0012524 might play important roles in the development and progression of SONFH; furthermore, valine, leucine, and isoleucine biosynthesis; ECM-receptor interaction; protein digestion and absorption potentially contributed to SONFH development. These

identified genes pathways may provide a more detailed molecular mechanism underlying SONFH development and progression, and hold promise as potential biomarkers and therapeutic targets. However, further studies are required to confirm the present results.

Author contributions

Conceptualization: Tao Yao, Zong-Sheng Yin, Wei Huang, Zhen-Fei Ding, Chao Cheng.

Data curation: Tao Yao, Zong-Sheng Yin, Wei Huang, Zhen-Fei Ding, Chao Cheng.

Formal analysis: Zong-Sheng Yin, Wei Huang, Zhen-Fei Ding, Chao Cheng.

Funding acquisition: Zong-Sheng Yin.

Methodology: Tao Yao, Zong-Sheng Yin, Wei Huang, Zhen-Fei Ding, Chao Cheng.

Writing – original draft: Tao Yao.

Writing – review and editing: Zong-Sheng Yin.

References

- [1] Mont MA, Cherian JJ, Sierra RJ, et al. Nontraumatic osteonecrosis of the femoral head: where do we stand today? A ten-year update. *J Bone Joint Surg Am* 2015;97:1604–27.
- [2] Moya-Angeler J, Gianakos AL, Villa JC, et al. Current concepts on osteonecrosis of the femoral head. *World J Orthop* 2015;6:590–601.
- [3] Al-Jabri T, Tan JYQ, Tong GY, et al. The role of electrical stimulation in the management of avascular necrosis of the femoral head in adults: a systematic review. *BMC Musculoskelet Disord* 2017;18:319.
- [4] Su W, Xu M, Chen X, et al. Long noncoding rna zeb1-as1 epigenetically regulates the expressions of zeb1 and downstream molecules in prostate cancer. *Mol Cancer* 2017;16:142.
- [5] Microsurgery Department of the Orthopedics Branch of the Chinese Medical Doctor A, Group from the Osteonecrosis and Bone Defect Branch of the Chinese Association of Reparative and Reconstructive Surgery, Microsurgery and Reconstructive Surgery Group of the Orthopedics Branch of the Chinese Medical Association . Chinese guideline for the diagnosis and treatment of osteonecrosis of the femoral head in adults. *Orthop Surg* 2017;9:3–12.
- [6] Kerachian MA, Seguin C, Harvey EJ. Glucocorticoids in osteonecrosis of the femoral head: a new understanding of the mechanisms of action. *J Steroid Biochem Mol Biol* 2009;114:121–8.
- [7] Weinstein RS. Clinical practice. Glucocorticoid-induced bone disease. *N Engl J Med* 2011;365:62–70.
- [8] Pennisi E. Genomics. Encode project writes eulogy for junk DNA. *Science* 2012;337:1159–61.
- [9] Arner E, Daub CO, Vitting-Seerup K, et al. Transcribed enhancers lead waves of coordinated transcription in transitioning mammalian cells. *Science* 2015;347:1010–4.
- [10] Schlosser K, Hanson J, Villeneuve PJ, et al. Assessment of circulating lncrnas under physiologic and pathologic conditions in humans reveals potential limitations as biomarkers. *Sci Rep* 2016;6:36596.
- [11] Wang Q, Yang Q, Chen G, et al. Lncrna expression profiling of bmscs in osteonecrosis of the femoral head associated with increased adipogenic and decreased osteogenic differentiation. *Sci Rep* 2018; 8:9127.
- [12] Chen J, Li Y, Zheng Q, et al. Circular rna profile identifies circpvt1 as a proliferative factor and prognostic marker in gastric cancer. *Cancer Lett* 2017;388:208–19.
- [13] Wang K, Long B, Liu F, et al. A circular rna protects the heart from pathological hypertrophy and heart failure by targeting mir-223. *Eur Heart J* 2016;37:2602–11.
- [14] Yuan HF, Christina VR, Guo CA, et al. Involvement of microRNA-210 demethylation in steroid-associated osteonecrosis of the femoral head. *Sci Rep* 2016;6:20046.
- [15] Kulcheski FR, Christoff AP, Margis R. Circular rnas are mirna sponges and can be used as a new class of biomarker. *J Biotechnol* 2016;238: 42–51.
- [16] Kerachian MA, Cournoyer D, Harvey EJ, et al. New insights into the pathogenesis of glucocorticoid-induced avascular necrosis: microarray analysis of gene expression in a rat model. *Arthritis Res Ther* 2010;12: R124.
- [17] Wang B, Su Y, Yang Q, et al. Overexpression of long non-coding rna hotair promotes tumor growth and metastasis in human osteosarcoma. *Mol Cells* 2015;38:432–40.
- [18] Wang A, Ren M, Song Y, et al. MicroRNA expression profiling of bone marrow mesenchymal stem cells in steroid-induced osteonecrosis of the femoral head associated with osteogenesis. *Med Sci Monit* 2018;24: 1813–25.
- [19] Li Z, Jiang C, Li X, et al. Circulating microRNA signature of steroid-induced osteonecrosis of the femoral head. *Cell Prolif* 2018;51: doi: 10.1111/cpr.12418. Epub 2017 Dec 4.
- [20] Li P, Zhai P, Ye Z, et al. Differential expression of mir-195-5p in collapse of steroid-induced osteonecrosis of the femoral head. *Oncotarget* 2017;8:42638–47.
- [21] Deng P, Zeng J, Li J, et al. Screening of serum protein markers for avascular osteonecrosis of femoral head differentially expressed after treatment with yuanshi shengmai chenggu tablets. *Biomed Res Int* 2018;2018:5692735.
- [22] Sakamoto Y, Yamamoto T, Sugano N, et al. Genome-wide association study of idiopathic osteonecrosis of the femoral head. *Sci Rep* 2017;7: 15035.
- [23] Baek SH, Kim KI, Yoon KS, et al. Genome-wide association scans for idiopathic osteonecrosis of the femoral head in a Korean population. *Mol Med Rep* 2017;15:750–8.